

## A Search for the Rare Leptonic Decays

$$B^+ \rightarrow \mu^+ \nu_\mu \text{ and } B^+ \rightarrow e^+ \nu_e$$

Belle Collaboration

N. Satoyama<sup>an</sup>, K. Abe<sup>i</sup>, I. Adachi<sup>i</sup>, H. Aihara<sup>au</sup>, D. Anipko<sup>a</sup>,  
A. M. Bakich<sup>ap</sup>, E. Barberio<sup>v</sup>, I. Bedny<sup>a</sup>, K. Belous<sup>ℓ</sup>,  
U. Bitenc<sup>o</sup>, I. Bizjak<sup>o</sup>, A. Bondar<sup>a</sup>, A. Bozek<sup>ab</sup>, M. Bračko<sup>i,u,o</sup>,  
T. E. Browder<sup>h</sup>, M.-C. Chang<sup>f</sup>, P. Chang<sup>aa</sup>, A. Chen<sup>y</sup>,  
W. T. Chen<sup>y</sup>, B. G. Cheon<sup>c</sup>, R. Chistov<sup>n</sup>, Y. Choi<sup>ao</sup>,  
Y. K. Choi<sup>ao</sup>, S. Cole<sup>ap</sup>, J. Dalseno<sup>v</sup>, M. Dash<sup>az</sup>,  
A. Drutskoy<sup>d</sup>, S. Eidelman<sup>a</sup>, S. Fratina<sup>o</sup>, N. Gabyshev<sup>a</sup>,  
T. Gershon<sup>i</sup>, A. Go<sup>y</sup>, G. Gokhroo<sup>aq</sup>, H. Ha<sup>q</sup>, J. Haba<sup>i</sup>,  
Y. Hasegawa<sup>an</sup>, K. Hayasaka<sup>w</sup>, D. Heffernan<sup>ag</sup>, T. Hokuue<sup>w</sup>,  
Y. Hoshi<sup>as</sup>, S. Hou<sup>y</sup>, W.-S. Hou<sup>aa</sup>, T. Iijima<sup>w</sup>, K. Ikado<sup>w</sup>,  
K. Inami<sup>w</sup>, A. Ishikawa<sup>au</sup>, R. Itoh<sup>i</sup>, M. Iwasaki<sup>au</sup>, Y. Iwasaki<sup>i</sup>,  
J. H. Kang<sup>ba</sup>, S. U. Kataoka<sup>x</sup>, N. Katayama<sup>i</sup>, H. Kawai<sup>b</sup>,  
T. Kawasaki<sup>ad</sup>, H. R. Khan<sup>av</sup>, H. Kichimi<sup>i</sup>, H. J. Kim<sup>r</sup>,  
S. K. Kim<sup>am</sup>, Y. J. Kim<sup>g</sup>, K. Kinoshita<sup>d</sup>, S. Korpar<sup>u,o</sup>,  
P. Križan<sup>t,o</sup>, P. Krokovny<sup>i</sup>, R. Kumar<sup>ah</sup>, C. C. Kuo<sup>y</sup>,  
A. Kuzmin<sup>a</sup>, Y.-J. Kwon<sup>ba</sup>, J. S. Lange<sup>e</sup>, G. Leder<sup>m</sup>,  
M. J. Lee<sup>am</sup>, T. Lesiak<sup>ab</sup>, A. Limosani<sup>i</sup>, S.-W. Lin<sup>aa</sup>,  
D. Liventsev<sup>n</sup>, G. Majumder<sup>aq</sup>, T. Matsumoto<sup>aw</sup>, S. McOnie<sup>ap</sup>,  
H. Miyake<sup>ag</sup>, H. Miyata<sup>ad</sup>, Y. Miyazaki<sup>w</sup>, R. Mizuk<sup>n</sup>,  
T. Mori<sup>w</sup>, T. Nagamine<sup>at</sup>, I. Nakamura<sup>i</sup>, E. Nakano<sup>af</sup>,  
M. Nakao<sup>i</sup>, H. Nakazawa<sup>y</sup>, Z. Natkaniec<sup>ab</sup>, S. Nishida<sup>i</sup>,  
O. Nitoh<sup>ay</sup>, S. Noguchi<sup>x</sup>, T. Nozaki<sup>i</sup>, S. Ogawa<sup>ar</sup>,  
T. Ohshima<sup>w</sup>, S. Okuno<sup>p</sup>, Y. Onuki<sup>aj</sup>, H. Ozaki<sup>i</sup>, P. Pakhlov<sup>n</sup>,  
G. Pakhlova<sup>n</sup>, H. Park<sup>r</sup>, R. Pestotnik<sup>o</sup>, L. E. Piilonen<sup>az</sup>,  
H. Sahoo<sup>h</sup>, Y. Sakai<sup>i</sup>, T. Schietinger<sup>s</sup>, O. Schneider<sup>s</sup>,  
J. Schümann<sup>z</sup>, C. Schwanda<sup>m</sup>, R. Seidl<sup>j,aj</sup>, K. Senyo<sup>w</sup>,

M. E. Sevier<sup>v</sup>, M. Shapkin<sup>ℓ</sup>, H. Shibuya<sup>ar</sup>, B. Shwartz<sup>a</sup>,  
 J. B. Singh<sup>ah</sup>, A. Sokolov<sup>ℓ</sup>, A. Somov<sup>d</sup>, N. Soni<sup>ah</sup>, S. Stanič<sup>ae</sup>,  
 M. Starič<sup>o</sup>, H. Stoeck<sup>ap</sup>, K. Sumisawa<sup>i</sup>, T. Sumiyoshi<sup>aw</sup>,  
 S. Suzuki<sup>ak</sup>, F. Takasaki<sup>i</sup>, K. Tamai<sup>i</sup>, N. Tamura<sup>ad</sup>,  
 M. Tanaka<sup>i</sup>, G. N. Taylor<sup>v</sup>, Y. Teramoto<sup>af</sup>, X. C. Tian<sup>ai</sup>,  
 I. Tikhomirov<sup>n</sup>, T. Tsuboyama<sup>i</sup>, T. Tsukamoto<sup>i</sup>, S. Uehara<sup>i</sup>,  
 T. Uglov<sup>n</sup>, S. Uno<sup>i</sup>, P. Urquijo<sup>v</sup>, G. Varner<sup>h</sup>, S. Villa<sup>s</sup>,  
 C. C. Wang<sup>aa</sup>, C. H. Wang<sup>z</sup>, M.-Z. Wang<sup>aa</sup>, Y. Watanabe<sup>av</sup>,  
 R. Wedd<sup>v</sup>, E. Won<sup>q</sup>, Q. L. Xie<sup>k</sup>, B. D. Yabsley<sup>ap</sup>,  
 A. Yamaguchi<sup>at</sup>, Y. Yamashita<sup>ac</sup>, M. Yamauchi<sup>i</sup>,  
 Z. P. Zhang<sup>al</sup>, V. Zhilich<sup>a</sup>, and A. Zupanc<sup>o</sup>,

<sup>a</sup>*Budker Institute of Nuclear Physics, Novosibirsk, Russia*

<sup>b</sup>*Chiba University, Chiba, Japan*

<sup>c</sup>*Chonnam National University, Kwangju, South Korea*

<sup>d</sup>*University of Cincinnati, Cincinnati, OH, USA*

<sup>e</sup>*University of Frankfurt, Frankfurt, Germany*

<sup>f</sup>*Department of Physics, Fu Jen Catholic University, Taipei, Taiwan*

<sup>g</sup>*The Graduate University for Advanced Studies, Hayama, Japan*

<sup>h</sup>*University of Hawaii, Honolulu, HI, USA*

<sup>i</sup>*High Energy Accelerator Research Organization (KEK), Tsukuba, Japan*

<sup>j</sup>*University of Illinois at Urbana-Champaign, Urbana, IL, USA*

<sup>k</sup>*Institute of High Energy Physics, Chinese Academy of Sciences, Beijing, PR  
China*

<sup>ℓ</sup>*Institute for High Energy Physics, Protvino, Russia*

<sup>m</sup>*Institute of High Energy Physics, Vienna, Austria*

<sup>n</sup>*Institute for Theoretical and Experimental Physics, Moscow, Russia*

<sup>o</sup>*J. Stefan Institute, Ljubljana, Slovenia*

<sup>p</sup>*Kanagawa University, Yokohama, Japan*

<sup>q</sup>*Korea University, Seoul, South Korea*

<sup>r</sup>*Kyungpook National University, Taegu, South Korea*

<sup>s</sup>*Swiss Federal Institute of Technology of Lausanne, EPFL, Lausanne, Switzerland*

<sup>t</sup>*University of Ljubljana, Ljubljana, Slovenia*

<sup>u</sup>*University of Maribor, Maribor, Slovenia*

<sup>v</sup>*University of Melbourne, Victoria, Australia*

<sup>w</sup>*Nagoya University, Nagoya, Japan*

<sup>x</sup>*Nara Women's University, Nara, Japan*

- <sup>y</sup> *National Central University, Chung-li, Taiwan*
- <sup>z</sup> *National United University, Miao Li, Taiwan*
- <sup>aa</sup> *Department of Physics, National Taiwan University, Taipei, Taiwan*
- <sup>ab</sup> *H. Niewodniczanski Institute of Nuclear Physics, Krakow, Poland*
- <sup>ac</sup> *Nippon Dental University, Niigata, Japan*
- <sup>ad</sup> *Niigata University, Niigata, Japan*
- <sup>ae</sup> *University of Nova Gorica, Nova Gorica, Slovenia*
- <sup>af</sup> *Osaka City University, Osaka, Japan*
- <sup>ag</sup> *Osaka University, Osaka, Japan*
- <sup>ah</sup> *Panjab University, Chandigarh, India*
- <sup>ai</sup> *Peking University, Beijing, PR China*
- <sup>aj</sup> *RIKEN BNL Research Center, Brookhaven, NY, USA*
- <sup>ak</sup> *Saga University, Saga, Japan*
- <sup>al</sup> *University of Science and Technology of China, Hefei, PR China*
- <sup>am</sup> *Seoul National University, Seoul, South Korea*
- <sup>an</sup> *Shinshu University, Nagano, Japan*
- <sup>ao</sup> *Sungkyunkwan University, Suwon, South Korea*
- <sup>ap</sup> *University of Sydney, Sydney, NSW, Australia*
- <sup>aq</sup> *Tata Institute of Fundamental Research, Bombay, India*
- <sup>ar</sup> *Toho University, Funabashi, Japan*
- <sup>as</sup> *Tohoku Gakuin University, Tagajo, Japan*
- <sup>at</sup> *Tohoku University, Sendai, Japan*
- <sup>au</sup> *Department of Physics, University of Tokyo, Tokyo, Japan*
- <sup>av</sup> *Tokyo Institute of Technology, Tokyo, Japan*
- <sup>aw</sup> *Tokyo Metropolitan University, Tokyo, Japan*
- <sup>ay</sup> *Tokyo University of Agriculture and Technology, Tokyo, Japan*
- <sup>az</sup> *Virginia Polytechnic Institute and State University, Blacksburg, VA, USA*
- <sup>ba</sup> *Yonsei University, Seoul, South Korea*

---

## Abstract

We present a search for the decays  $B^+ \rightarrow \mu^+\nu_\mu$  and  $B^+ \rightarrow e^+\nu_e$  in a  $253\text{ fb}^{-1}$  data sample collected at the  $\Upsilon(4S)$  resonance with the Belle detector at the KEKB asymmetric-energy  $B$  factory. We find no significant evidence for a signal and set 90% confidence level upper limits of  $\mathcal{B}(B^+ \rightarrow \mu^+\nu_\mu) < 1.7 \times 10^{-6}$  and  $\mathcal{B}(B^+ \rightarrow e^+\nu_e) < 9.8 \times 10^{-7}$ .

## 1 Introduction

The purely leptonic decay  $B^+ \rightarrow \ell^+ \nu_\ell$  (charge conjugate states are implied throughout the paper) is of particular interest since it provides a direct measurement of the product of the magnitude of the Cabibbo-Kobayashi-Maskawa matrix element,  $|V_{ub}|$  [1], and the  $B$  meson decay constant,  $f_B$ . In the Standard Model (SM) the branching fraction of the decay  $B^+ \rightarrow \ell^+ \nu_\ell$  is given as

$$\mathcal{B}(B^+ \rightarrow \ell^+ \nu_\ell) = \frac{G_F^2 m_B m_\ell^2}{8\pi} \left(1 - \frac{m_\ell^2}{m_B^2}\right)^2 f_B^2 |V_{ub}|^2 \tau_B, \quad (1)$$

where  $G_F$  is the Fermi coupling constant,  $m_\ell$  and  $m_B$  are the charged lepton and  $B$  meson masses, and  $\tau_B$  is the  $B^+$  lifetime. The expected branching fractions are  $(4.7 \pm 0.7) \times 10^{-7}$  for  $B^+ \rightarrow \mu^+ \nu_\mu$  and  $(1.1 \pm 0.2) \times 10^{-11}$  for  $B^+ \rightarrow e^+ \nu_e$  assuming  $|V_{ub}| = (4.39 \pm 0.33) \times 10^{-3}$  determined from inclusive charmless semileptonic  $B$  decay data [2],  $\tau_B = 1.643 \pm 0.010$  ps [2], and  $f_B = 0.216 \pm 0.022$  GeV obtained from lattice QCD calculations [3]. However, non-SM physics could yield larger branching fractions [4].

The Belle experiment has recently found the first evidence for the purely leptonic decay  $B^+ \rightarrow \tau^+ \nu_\tau$  [5]. The other purely leptonic  $B$  decays,  $B^+ \rightarrow \mu^+ \nu_\mu$  and  $B^+ \rightarrow e^+ \nu_e$ , have not yet been observed. The most stringent current upper limits for these modes are  $\mathcal{B}(B^+ \rightarrow \mu^+ \nu_\mu) < 6.6 \times 10^{-6}$  [6] and  $\mathcal{B}(B^+ \rightarrow e^+ \nu_e) < 1.5 \times 10^{-5}$  [7]. Preliminary limits of  $\mathcal{B}(B^+ \rightarrow \mu^+ \nu_\mu) < 2.0 \times 10^{-6}$  [8] and  $\mathcal{B}(B^+ \rightarrow e^+ \nu_e) < 7.9 \times 10^{-6}$  [9] are also available from the Belle and BaBar collaborations, respectively. In this paper, we present a search for the decays  $B^+ \rightarrow \mu^+ \nu_\mu$  and  $B^+ \rightarrow e^+ \nu_e$ .

## 2 Data Set and Experiment

The data used in this analysis were collected with the Belle detector at the KEKB asymmetric-energy  $e^+e^-$  collider [10]. The sample has an integrated luminosity of  $253 \text{ fb}^{-1}$  accumulated at the  $\Upsilon(4S)$  resonance, at a center-of-mass (CM) energy of 10.58 GeV (on-resonance), and  $28.1 \text{ fb}^{-1}$  accumulated at a CM energy 60 MeV below the  $\Upsilon(4S)$  resonance (off-resonance).

The Belle detector is a large solid-angle spectrometer based on a 1.5 T superconducting solenoid magnet. Charged particle tracking and momentum measurements are made with a three-layer, double-sided silicon vertex detector (SVD) and a central drift chamber (CDC). Identification of charged hadrons is provided by a combination of three measurements: specific ionization loss ( $dE/dx$ ) in the CDC, photon yield in the aerogel threshold Cherenkov counters (ACC), and time-of-flight information from a cylindrical array of 128 scintillation counters (TOF). Photons are detected in an electromagnetic calorimeter (ECL) system made of an array of 8736 CsI(Tl) crystals surrounding the TOF system. The ECL is also used for electron identification. Muons are identified by a resistive plate chamber system (KLM) located within the solenoid's external return yoke.

Particle identification for  $e^\pm$  and  $\mu^\pm$  is important for this analysis. Electron identification is based on the ratio of the cluster energy in the ECL to the track momentum from the CDC and the SVD ( $E/p$ ), the  $dE/dx$  in the CDC, the position and shower shape of the cluster in the ECL and the response from the ACC. Muon identification is based on the hit positions and the depth of penetration into the KLM. The efficiency of electron identification is over 90 % in the momentum range of this analysis while the misidentification rate is below 0.5 %. The muon identification efficiency is approximately 85 % in the momentum range of this analysis with a misidentification rate of approximately 1 %. The Belle detector is described in detail elsewhere [11].

A detailed Monte Carlo (MC) simulation, which fully describes the detector geometry and response based on GEANT [12], is used to estimate the signal detection efficiency and to study the background. The MC samples are produced with the EvtGen event generator [13].

### 3 Signal Selection

We search for events in which there is one well-identified lepton. The signal candidate muon or electron is required to pass tight particle identification requirements; lepton candidates that can be associated to other tracks in the event to reconstruct  $K_S^0$  mesons or photon conversions are explicitly vetoed. Signal lepton candidates are required to originate from the interaction point (IP) and to have their polar angle,  $\theta_\ell$ , formed by the lepton momentum with the detector axis (opposite to the direction of the positron beam), in the range  $-0.5 < \cos \theta_\ell < 0.8$  for muons and  $-0.50 < \cos \theta_\ell < 0.85$  for electrons.

As  $B^+ \rightarrow \ell^+ \nu_\ell$  is a two-body decay, the lepton has a fixed momentum in the signal  $B$  meson ( $B^{\text{sig}}$ ) rest frame, with  $p_\ell^B$  equal to approximately half of the  $B$  meson mass,  $p_\ell^B \sim m_B/2$ . The lepton momentum in the CM frame,  $p_\ell^*$ , is

related to  $p_\ell^B$  by

$$p_\ell^B \simeq p_\ell^* \left( 1 - \frac{|\vec{p}_{B^{\text{sig}}}^*|}{m_B} \cos \theta_{\ell-B^{\text{sig}}} \right) \quad (2)$$

where  $\vec{p}_{B^{\text{sig}}}^*$  is the momentum of the  $B^{\text{sig}}$  in the CM frame and  $\cos \theta_{\ell-B^{\text{sig}}}$  represents the cosine of the angle between the directions of the signal lepton and  $B^{\text{sig}}$  in the CM frame.

Since the neutrino is not detected in the  $B^{\text{sig}}$  decay, we obtain  $\vec{p}_{B^{\text{sig}}}^*$  by inclusive reconstruction of the companion  $B$  meson ( $B^{\text{comp}}$ ) recoiling against  $B^{\text{sig}}$ . For the  $B^{\text{comp}}$  reconstruction, we use all detected photons and charged tracks, except for the signal lepton candidate.  $K_S^0 \rightarrow \pi^+\pi^-$  and  $\gamma \rightarrow e^+e^-$  decays are fully reconstructed, in order to correctly account for the momentum of tracks originating from vertices displaced from the IP. The missing momentum in the laboratory frame that is calculated by using all photons, charged tracks, and the signal lepton, is assigned to the neutrino. The quantity  $|\vec{p}_{B^{\text{sig}}}^*|$  is approximately given by  $\sqrt{E_{\text{beam}}^2 - m_B^2} \simeq 0.32 \text{ GeV}/c$  using the beam energy in the CM frame ( $E_{\text{beam}}$ ), while  $\cos \theta_{\ell-B^{\text{sig}}}$  is related to the angle between the direction of the signal lepton and the momentum of  $B^{\text{comp}}$  ( $\theta_{\ell-B^{\text{comp}}}$ ) by  $\cos \theta_{\ell-B^{\text{sig}}} = -\cos \theta_{\ell-B^{\text{comp}}}$ . Thus, equation 2 can be expressed in terms of two measurable quantities,  $p_\ell^*$  and  $\cos \theta_{\ell-B^{\text{comp}}}$ :

$$p_\ell^B \simeq p_\ell^* (1 + 0.06 \cos \theta_{\ell-B^{\text{comp}}}). \quad (3)$$

Signal candidates are selected using the kinematic variables  $M_{bc} = \sqrt{E_{\text{beam}}^2 - |\vec{p}_B^*|^2}$  and  $\Delta E = E_B^* - E_{\text{beam}}$ , where  $\vec{p}_B^*$  and  $E_B^*$  are the momentum and energy of  $B^{\text{comp}}$ , all variables being evaluated in the CM frame. Events in the *fit region* that satisfy  $5.10 \text{ GeV}/c^2 < M_{bc} < 5.29 \text{ GeV}/c^2$  and  $-0.8 (-1.0) \text{ GeV} < \Delta E < 0.4 \text{ GeV}$  for the muon (electron) mode are kept for further analysis. A more restricted *signal region* is also defined by the same requirements on  $\Delta E$  and by  $M_{bc} > 5.26 \text{ GeV}/c^2$ .

The dominant background arises from the continuum process  $e^+e^- \rightarrow q\bar{q}$  ( $q = u, d, s, c$ ) and semileptonic  $B$  meson decays, mostly into charm final states ( $B \rightarrow X_c \ell \nu$ ) with contributions from rare  $b \rightarrow u$  modes ( $B \rightarrow X_u \ell \nu$ ). The missing momentum of continuum events is often due to undetected particles that are outside the detector acceptance. In order to reduce such backgrounds, we require the transverse component of the missing momentum to be greater than  $1.75 \text{ GeV}/c$ , and the cosine of the polar angle to be less than  $0.84$  ( $0.82$ ) for the muon (electron) mode, respectively.

Figure 1 shows the measured  $p_\ell^B$  distributions after reconstruction of the companion  $B$  meson. We require  $2.6 \text{ GeV}/c < p_\mu^B < 2.84 \text{ GeV}/c$  and  $2.6 \text{ GeV}/c <$

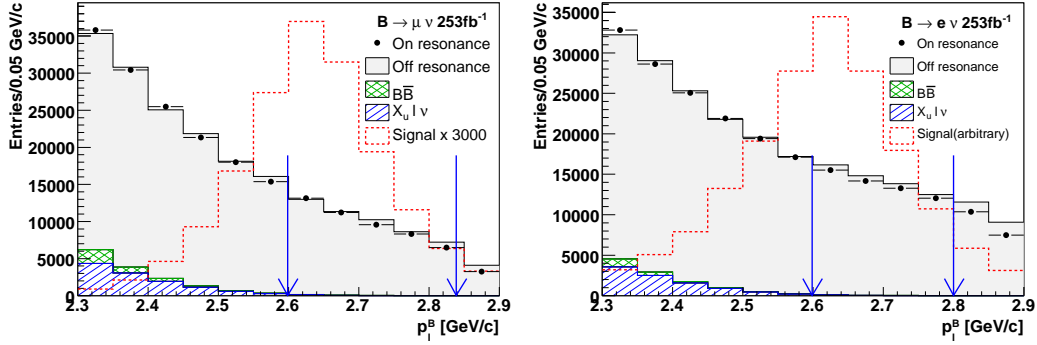


Fig. 1. Lepton momentum distributions in the rest frame of the signal  $B$  meson for the muon (left) and electron (right) mode after reconstruction of the companion  $B$  meson. Points show the on-resonance data, and solid histograms show the expected background due to rare  $B \rightarrow X_u \ell \nu$  decays (hatched, from MC); other  $B\bar{B}$  events, principally  $B \rightarrow X_c \ell \nu$  decays (cross-hatched, also from MC); and continuum events (light shaded, taken from scaled off-resonance data). The dashed histograms represent the signal as predicted by the MC with arbitrary normalization.

$p_e^B < 2.8 \text{ GeV}/c$  for the signal candidates. This requirement removes most of the  $B \rightarrow X_c \ell \nu$  background.

In order to further suppress the continuum background we exploit the event shape difference between continuum events, which are jet-like, and  $B\bar{B}$  events, which tend to have a more spherical topology. Modified Fox-Wolfram moments [14,15] are combined into a Fisher discriminant ( $F$ ). Figure 2 shows the Fisher discriminant distributions for events that passed the  $\cos\theta_\ell$  selection. We require  $F > 0.3$  for the muon mode and  $F > 0$  for the electron mode, which retain approximately 51% (60%) of the signal in the signal region and remove approximately 99% (95%) of the continuum background in the signal region for the muon (electron) mode.

We determine all selection criteria by maximizing  $N_S/\sqrt{N_S + N_B}$ , where  $N_S$  is the number of signal events expected in the signal region computed assuming the SM branching fractions and  $N_B$  is the number of expected background events in the signal region from MC.

After all selection criteria have been applied, the signal selection efficiency in the signal region is estimated to be  $\epsilon_\mu = 2.18 \pm 0.06\%$  for the muon mode and  $\epsilon_e = 2.39 \pm 0.06\%$  for the electron mode. The efficiencies in the fit region are  $3.15 \pm 0.07\%$  for the muon mode and  $3.86 \pm 0.08\%$  for the electron mode. Figure 3 shows the  $p_\ell^B$  distributions after all other selections have been applied. The background that remains in the signal region consists of approximately 76% continuum and 24%  $B \rightarrow X_u \ell \nu$  according to the off-resonance data and MC studies. The MC study also indicates that the latter exhibits a peaking  $M_{bc}$  distribution with significantly larger width than the signal distribution.

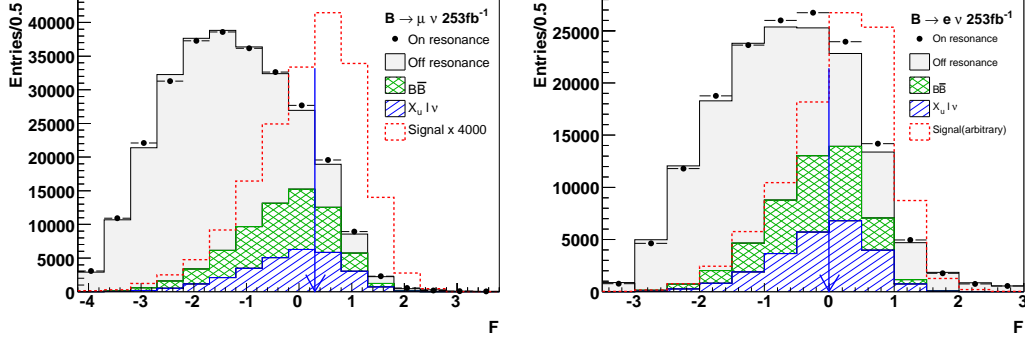


Fig. 2. Fisher discriminant distributions for the muon (left) and electron (right) mode after  $\cos\theta_\ell$  requirements have been applied. Points show the on-resonance data, and solid histograms show the expected background due to rare  $B \rightarrow X_u \ell \nu$  decays (hatched, from MC); other  $B\bar{B}$  events, principally  $B \rightarrow X_c \ell \nu$  decays (cross-hatched, also from MC); and continuum events (light shaded, taken from scaled off-resonance data). The dashed histograms represent the signal as predicted by the MC with arbitrary normalization.

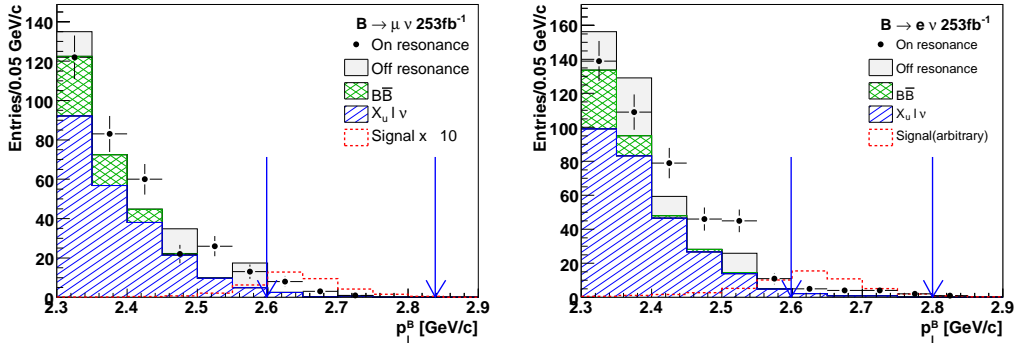


Fig. 3.  $p_\ell^B$  distributions for the signal candidates. Points show the on-resonance data, and solid histograms show the expected background due to rare  $B \rightarrow X_u \ell \nu$  decays (hatched, from MC); other  $B\bar{B}$  events, principally  $B \rightarrow X_c \ell \nu$  decays (cross-hatched, also from MC); and continuum events (light shaded, taken from scaled off-resonance data). Dashed histograms are MC  $B \rightarrow \ell \nu$  signals that are obtained by multiplying the SM expectations by a factor of 10 for the muon mode and by  $5 \times 10^6$  for the electron mode. The arrows show the signal regions.

## 4 Signal Extraction

The signal yields are extracted from unbinned maximum likelihood fits to  $M_{bc}$  distributions in the fit region. The signal  $M_{bc}$  distribution is parameterized by a Crystal Ball function [16] modeled on the signal MC. The background is described by ARGUS functions [17], with shape parameters determined from the off-resonance data for the continuum background and from MC for the  $B\bar{B}$  background. We do not include the peaking component from  $B \rightarrow X_u \ell \nu$  in this fit since an examination of  $\Delta E$  sideband data indicates that the peaking contribution is negligible. The expected number of background events in the



	Muon Mode	Electron Mode
Signal Efficiency (fit region)	$3.15 \pm 0.07 \%$	$3.86 \pm 0.08 \%$
Signal Efficiency (signal region)	$2.18 \pm 0.06 \%$	$2.39 \pm 0.06 \%$
Observed in Signal region [events]	12	15
Expected background [events]	$7.4 \pm 1.0$	$13.4 \pm 1.4$
Signal yield [events]	$4.1 \pm 3.1$	$-1.8 \pm 3.3$
Significance	1.3	–
SM Prediction [events]	$2.8 \pm 0.2$	$(7.3 \pm 1.4) \times 10^{-5}$

Table 1

Selection efficiencies, expected numbers of events for signal and background and fit results.

signal region is estimated by fitting the  $M_{bc}$  distribution outside the signal region to a background shape determined from the  $B\bar{B}$  MC and off-resonance data. The expected number of background events is  $7.4 \pm 1.0$  ( $13.4 \pm 1.4$ ) for the muon (electron) mode. Use of the combination of the  $B\bar{B}$  MC samples and off-resonance data instead of the on-resonance data gives similar expected number of background events. The  $M_{bc}$  distributions are used as probability density functions (PDF) to compute an extended likelihood function defined as follows:

$$\mathcal{L}(n_s, n_b) = \frac{e^{-(n_s+n_b)}}{N!} \prod_{i=1}^N (n_s f_s(i) + n_b f_b(i)) \quad (4)$$

where  $n_s$  and  $n_b$  represent the numbers of signal and background events in the fit region to be determined in the fit,  $N$  is the number of observed events,  $f_s$  and  $f_b$  are the signal and background PDFs, respectively. The negative log likelihood function is minimized using MINUIT [18] with two free parameters  $n_b$  and  $n_s$  where  $n_s = \epsilon_\ell \times N_{B\bar{B}} \times \mathcal{B}(B^+ \rightarrow \ell^+ \nu)$  with  $\epsilon_\ell$  being the efficiency in the fit region, and  $N_{B\bar{B}}$  the total number of  $B\bar{B}$  events analysed. We assume the number of the charged and neutral  $B\bar{B}$  pairs to be equal.

Figure 4 shows the  $M_{bc}$  distributions of events in the  $\Delta E$  signal region together with the fit results. We observe 12 (15) events for the muon (electron) mode in the signal region. The signal yield extracted from the fit is  $4.1 \pm 3.1$  events for the muon mode and  $-1.8 \pm 3.3$  events for the electron mode in the signal region. For the SM branching fractions, we expect  $2.8 \pm 0.2$  and  $(7.3 \pm 1.4) \times 10^{-5}$  events for the muon mode and the electron mode, respectively. The significance of the signal in the muon mode is 1.3, which is defined as  $\sqrt{2 \ln(\mathcal{L}_{\max}/\mathcal{L}_0)}$  where  $\mathcal{L}_{\max}$  is the likelihood value for the best-fit signal yield and  $\mathcal{L}_0$  is the likelihood value for no signal event. No excess of events is observed in the electron mode. Selection efficiencies, expected numbers of events for signal and background and fit results are summarized in Table 1.

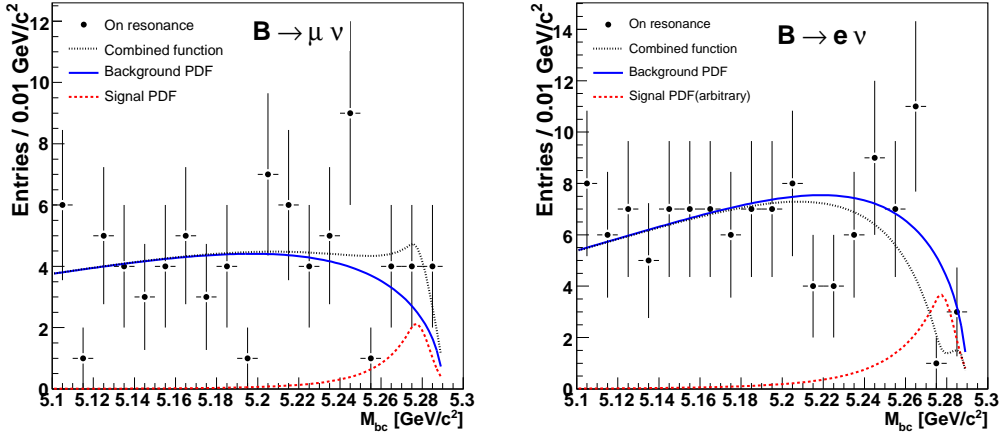


Fig. 4.  $M_{bc}$  distributions for the events in the  $\Delta E$  signal region, together with the fit results (dotted lines). The solid curves are the background contributions. The dashed curves are the signal contributions. The signal contribution in the electron mode is multiplied by a factor of  $-4$  to make it visible on the plot.

## 5 Systematic Uncertainties

The main sources of systematic uncertainty in calculating  $\mathcal{B}(B^+ \rightarrow \ell^+ \nu)$  arise from the uncertainties in the number of  $B^+ B^-$  events ( $N_{B\bar{B}} = (276.6 \pm 3.1) \times 10^6$ ), determination of the signal efficiency, and parameterization of the  $M_{bc}$  distribution for the signal and background. The uncertainty due to the number of  $B\bar{B}$  pairs is 1.1%. The uncertainties from the signal efficiencies are: 1% due to the uncertainties in the track-finding efficiency for the signal, 4.4% due to the uncertainty in the muon ID efficiency and 1.1% due to the electron ID efficiency, 2.3% (2.1%) for the muon (electron) mode from the MC statistics. We calculate an efficiency correction factor, to account for differences between MC and data, by analyzing a control data sample of fully reconstructed  $B^+ \rightarrow \bar{D}^{(*)0} \pi^+$  decays, where we treat the pion as a signal lepton and the  $\bar{D}^{(*)0}$  as the accompanying neutrino. The event topology is similar to that of the signal events as both are two-body decays. The companion  $B$  is reconstructed in the control data samples as in the signal sample. We compare the efficiencies of the control data sample and a corresponding MC sample and determine correction factors for the signal efficiencies. The correction factors obtained are  $1.01 \pm 0.04$  for the muon mode and  $1.13 \pm 0.04$  for the electron mode. We apply a correction only to the electron mode, while uncertainties on the correction factors contribute to the systematic uncertainties of both modes at the level of 3.6%.

The uncertainties related to the signal  $M_{bc}$  shapes are estimated by repeating the fits while varying the Crystal Ball function parameters by their uncertainties; their contribution is 6.5% for the muon mode and 3.2% for the electron

Sources		Muon Mode	Electron Mode
$N_{B\bar{B}}$		1.1%	1.1%
Signal Efficiency	Lepton ID	4.4%	1.1%
	Tracking	1.0%	1.0%
	MC statistics	2.3%	2.1%
	$B^+ \rightarrow D^0\pi^+$	3.6%	3.6%
$M_{bc}$ Shape	Signal	6.5%	3.2%
	Background	8.1%	15.7%
Total		12.2%	16.7%

Table 2

Summary of systematic uncertainties

mode. Uncertainties due to the background  $M_{bc}$  shapes are estimated in a similar manner by varying the ARGUS function parameters and yield 8.1 % for the muon mode and 15.7 % for the electron mode. Table 2 summarizes the contributions to the systematic uncertainties.

## 6 Limits on Branching Fractions

Figure 5 shows the dependence of the likelihood functions on the branching fractions,  $\mathcal{L}(B)$ , before and after inclusion of the systematic uncertainties. To account for systematic uncertainties in the calculation of the upper limits for each mode, we convolve the likelihood function  $\mathcal{L}(B)$  with a Gaussian distribution, where the sigma of the Gaussian corresponds to the size of the systematic uncertainty in this mode. The 90 % confidence level for the upper limit on the branching fraction,  $\mathcal{B}_{90}$ , is defined by  $0.9 = \int_0^{\mathcal{B}_{90}} \mathcal{L}(\mathcal{B})d\mathcal{B} / \int_0^\infty \mathcal{L}(\mathcal{B})d\mathcal{B}$ .

We obtain the following upper limits on the branching fractions at the 90 % confidence level:

$$\mathcal{B}(B^+ \rightarrow \mu^+\nu_\mu) < 1.7 \times 10^{-6} \quad (90\% \text{ C.L.}) \quad (5)$$

$$\mathcal{B}(B^+ \rightarrow e^+\nu_e) < 9.8 \times 10^{-7} \quad (90\% \text{ C.L.}), \quad (6)$$

including the effect of the systematic uncertainties. The expected sensitivities on the upper limits with the present dataset, computed using toy MC studies with a null signal hypothesis, are  $1.0 \times 10^{-6}$  for the muon mode and  $1.1 \times 10^{-6}$  for the electron mode.

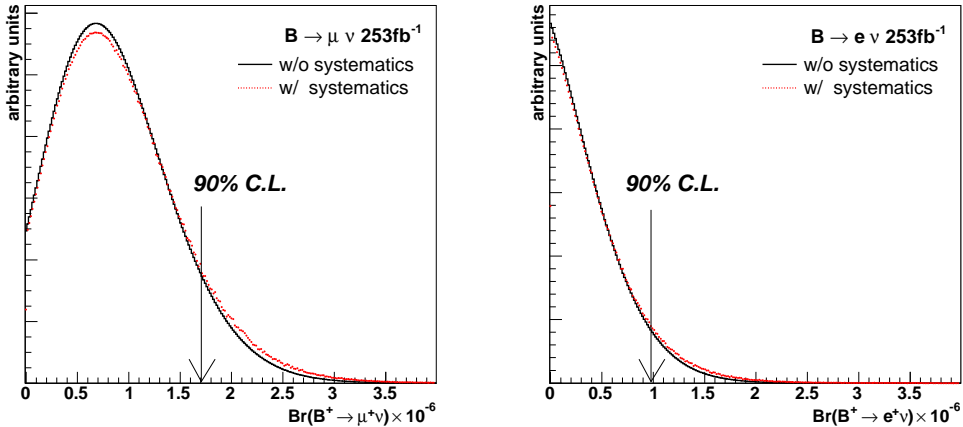


Fig. 5. Likelihood function dependence on the branching fractions. The solid and dotted curves represent the likelihood functions without and with inclusion of systematic uncertainties, respectively. The arrows indicate the upper limits on the branching fractions at 90% confidence level.

## 7 Conclusion

We have searched for the purely leptonic decays  $B^+ \rightarrow \mu^+ \nu_\mu$  and  $B^+ \rightarrow e^+ \nu_e$  using data collected by the Belle detector at the KEKB  $e^+e^-$  asymmetric-energy collider. We have found no evidence of signal in either decay mode. We set upper limits on the branching fractions:  $\mathcal{B}(B^+ \rightarrow \mu^+ \nu_\mu) < 1.7 \times 10^{-6}$  and  $\mathcal{B}(B^+ \rightarrow e^+ \nu_e) < 9.8 \times 10^{-7}$  at 90% confidence level. These limits are the most stringent to date and improve the previous published limits [6,7] by a factor of 4 for  $B^+ \rightarrow \mu^+ \nu_\mu$  and 15 for  $B^+ \rightarrow e^+ \nu_e$ .

We thank the KEKB group for the excellent operation of the accelerator, the KEK cryogenics group for the efficient operation of the solenoid, and the KEK computer group and the National Institute of Informatics for valuable computing and Super-SINET network support. We acknowledge support from the Ministry of Education, Culture, Sports, Science, and Technology of Japan and the Japan Society for the Promotion of Science; the Australian Research Council and the Australian Department of Education, Science and Training; the National Science Foundation of China and the Knowledge Innovation Program of the Chinese Academy of Sciences under contract No. 10575109 and IHEP-U-503; the Department of Science and Technology of India; the BK21 program of the Ministry of Education of Korea, the CHEP SRC program and Basic Research program (grant No. R01-2005-000-10089-0) of the Korea Science and Engineering Foundation, and the Pure Basic Research Group program of the Korea Research Foundation; the Polish State Committee for Scientific Research; the Ministry of Science and Technology of the Russian

Federation; the Slovenian Research Agency; the Swiss National Science Foundation; the National Science Council and the Ministry of Education of Taiwan; and the U.S. Department of Energy.

## References

- [1] N. Cabibbo, Phys. Rev. Lett. **10**, 531 (1963), see also M. Kobayashi and T. Maskawa, Prog. Theor. Phys. **49**, 652 (1973).
- [2] E. Barberio *et al.* (Heavy Flavor Averaging Group), hep-ex/0603003 (2006).
- [3] A. Gray *et al.* (HPQCD Collaboration), Phys. Rev. Lett. **95**, 212001 (2005). See also S. Hashimoto, Int. J. Mod. Phys. **A 20**, 5133 (2005), which quotes an average value of  $0.189 \pm 0.027$  GeV. QCD sum rules predict  $f_B = 210 \pm 19$  MeV, see M. Jamin and B. O. Lange, Phys. Rev. D **65**, 056005 (2002).
- [4] W. S. Hou, Phys. Rev. D **48**, 2342 (1993).
- [5] K. Ikado *et al.* (Belle Collaboration), Phys. Rev. Lett. **97**, 251802 (2006).
- [6] B. Aubert *et al.* (BaBar Collaboration), Phys. Rev. Lett. **92**, 221803 (2004).
- [7] M. Artuso *et al.* (CLEO Collaboration), Phys. Rev. Lett. **75**, 785 (1995).
- [8] K. Abe *et al.* (Belle Collaboration), hep-ex/0408132 (2004).
- [9] B. Aubert *et al.* (BaBar Collaboration), hep-ex/0607110 (2006).
- [10] S. Kurokawa and E. Kikutani, Nucl. Instrum. Meth. A **499**, 1 (2003), and other papers included in this volume.
- [11] A. Abashian *et al.* (Belle Collaboration), Nucl. Instrum. Meth. A **479**, 117 (2002).
- [12] R. Brun *et al.* GEANT3.21, CERN Report DD/EE/84-1 (1984).
- [13] D. J. Lange, Nucl. Instrum. Meth. A **462**, 152 (2001).
- [14] G. C. Fox and S. Wolfram, Phys. Rev. Lett. **41**, 1581 (1978).
- [15] K. Abe *et al.* (Belle Collaboration), Phys. Lett. B **511**, 151(2001).
- [16] E. D. Bloom and C. Peck, Ann. Rev. Nucl. Part. Sci. **33**, 143 (1983).
- [17] H. Albert *et al.* (ARGUS Collaboration), Phys. Lett. B **241**, 278 (1990).
- [18] F. James and M. Roos, Comput. Phys. Commun. **10**, 343 (1975).